Critical current behavior in Josephson junctions with the weak ferromagnet PdNi

Trupti S. Khaire, W. P. Pratt, Jr., and Norman O. Birge*
Department of Physics and Astronomy, Michigan State University, East Lansing, Michigan 48824-2320, USA
(Received 17 December 2008; revised manuscript received 25 February 2009; published 27 March 2009)

We have studied the variation in critical current in superconductor/ferromagnet/superconductor Josephson Junctions as a function of ferromagnet thickness using a weakly ferromagnetic alloy $Pd_{82}Ni_{12}$. Measurements were performed for the thickness range 32–100 nm, over which the critical current density decreases by 5 orders of magnitude. The critical current density oscillates with a period of $\pi\times(4.4\pm0.1)$ nm, and decays over a characteristic length of 7.7 ± 0.5 nm. There is no evidence of a crossover to a slower decay, which might indicate the presence of long-range spin-triplet pair correlations. We discuss possible reasons for their absence, including the possibility of strong spin-flip scattering in PdNi.

DOI: 10.1103/PhysRevB.79.094523 PACS number(s): 74.50.+r, 74.45.+c, 75.30.Gw, 74.20.Rp

I. INTRODUCTION

When a superconducting (S) metal is placed in contact with a normal (N) metal, the properties of both metals are modified near the S/N interface. The resulting superconducting proximity effect was widely studied in the 1960s,[1] and again in the 1990s.[2,3] When the normal metal is replaced by a ferromagnetic (F) metal, the resulting physics is extremely rich, due to the very different order parameters in the two metals. There has been sustained interest in S/F systems over at least the past decade.[4,5] Many new phenomena have been observed, including but not limited to: oscillations in the critical temperature of S/F bilayers as a function of F layer thickness,[6] variations in the critical temperature of F/S/F trilayers as a function of the relative magnetization direction of the two F layers,[7] and oscillations in the critical current of S/F/S Josephson junctions.[8] The oscillatory behaviors are a direct result of the exchange splitting of the spin-up and spin-down bands in the ferromagnet, which produce a momentum shift between the up- and down-spin electrons of a Cooper pair that "leaks" from S into F.[9] In the clean limit, the spatial period of the oscillations is governed by the exchange length, $\xi_F=\hbar v_F/2E_{ex}$, where v_F and E_{ex} are the Fermi velocity and exchange energy of the F material, respectively.

Unlike the S/N proximity effect, which extends to distances of order 1 μm at sufficiently low temperature, the novel phenomena associated with the S/F proximity effect persist only over very short distances—limited either by ξ_F, by the mean-free path, l_e, or by their geometric mean, the dirty-limit exchange length $\xi_F^*=\sqrt{(\hbar D/E_{ex})}$, where $D=v_F l_e/3$ is the diffusion constant. These distance scales, characterizing the oscillation and decay of superconducting correlations, tend to be extremely short in strong ferromagnets, and only moderately longer in the weakly ferromagnetic alloys preferred by some groups. For example, oscillations in the critical current in Nb/Co/Nb Josephson junctions have been observed with a period of 1.0 nm and a decay constant of 3.0 nm.[10] $InNb/Cu_{47}Ni_{53}/Nb$ alloy junctions, the observed period and decay constants were 11.0 and 1.3 nm, respectively.[8]

In this context, it was very exciting when two theoretical groups predicted that a new form of superconducting order, with spin-triplet pairing, could be induced by certain types of magnetic inhomogeneity in S/F systems consisting of conventional spin-singlet superconducting materials.[11–14] Cooper pair correlations with spin-triplet symmetry are not subject to the exchange field of the ferromagnetic, since both electrons in the pair enter the same spin band in the ferromagnet. As a result, proximity effects due to such correlations should persist over long distances in a ferromagnetic, limited either by the temperature or by spin-flip and spin-orbit scattering. Furthermore, the spin-triplet correlations predicted to occur in S/F systems are not of same type discovered recently in materials such as $SrRuO_4$.[15] In $SrRuO_4$, the spin-triplet Cooper pairs satisfy the spin-statistics theorem by having odd orbital angular momentum. In contrast, the spin-triplet correlations predicted to occur in S/F systems have even orbital angular momentum, and satisfy the spin-statistics theorem by virtue of being odd in time or frequency.[16]

Experimental confirmation of the presence of spin-triplet correlations is not easy. In retrospect, several theorists have suggested their role in old experiments performed on mesoscopic S/F hybrid samples, where the data were interpreted in terms of a long-range superconducting proximity effect.[17–19] More recently, there has been one report of a Josephson current in S/F/S structures using CrO_2 as the F material,[20] where the distance between the S layers was very long (several hundred nm), so that the conventional spin-singlet supercurrent should be exponentially suppressed. In a different work,[21] phase-coherent oscillations were observed in the normal resistance of a Ho wire connected to two superconducting electrodes, again separated by a distance too large to support spin-singlet correlations. In both cases, the data were interpreted as being due to spin-triplet superconducting correlations in the ferromagnetic material. While these pioneering experiments are highly suggestive and tantalizing, the first suffers from large sample-to-sample fluctuations in the magnitude of the observed supercurrent,[20] while both lack direct evidence for spin-triplet correlations.

The goal of this work is to study S/F/S Josephson junctions where the thickness of the F layer is increased systematically, from a thin regime where the supercurrent is likely to be dominated by spin-singlet correlations, to a thick regime where the smaller but longer-range spin-triplet supercurrent takes over. We chose Nb as the S material because its large critical temperature allows us to make measurements at 4.2 K, and hence measure a large number of samples. For the

F material, we chose $Pd_{1-x}Ni_x$ alloy with a Ni concentration of 12 at. %, a material studied extensively by the group of Aprili[22,23] and others,[24–28] but only with PdNi thicknesses less than 15 nm. Our choice of this particular weakly ferromagnetic alloy was based on two considerations: (1) using a weakly ferromagnetic material allows us to increase the thickness of the F layer without introducing an overwhelming amount of intrinsic magnetic flux inside the junctions. (This issue will be discussed further in Sec. III below.) (2) Some weakly ferromagnetic alloys suffer from strong spin-orbit and/or spin-flip scattering, which are likely to destroy both spin-singlet and spin-triplet correlations. For example, Ryazanov and co-workers[8,29] have found that the Josephson current in S/F/S junctions using $Cu_{1-x}Ni_x$ alloy with $x=53$ at. % decreases exponentially over a length scale of only 1.3 nm. Moreover, that length scale is much shorter than the one characterizing the critical current oscillations, a fact that implicates strong spin-flip scattering in CuNi alloy.[9,14,30] In contrast, while Kontos *et al.*[23] found that the critical current in S/F/S junctions made with PdNi alloy decays over a length scale only slightly longer, 2.8 nm, they found that the oscillations and decay are governed by the *same* length scale, which may imply that spin-flip and spin-orbit scattering are weak in this material.

The paper is organized as follows. In Sec. II we discuss sample fabrication methods and characterization of the PdNi alloy. Section III discusses the characterization of our S/F/S Josephson junctions, with particular attention to the magnetic-field dependence of the critical current (the so-called "Fraunhofer pattern"). Section IV presents the main results of the paper, namely, the critical current vs PdNi thickness of our S/F/S Josephson junctions. Section V discusses the various theoretical works on S/F/S junctions, and the physical parameters that one can extract from fitting theoretical formulas to the data. Our interpretation of the results is presented in Sec. VI. Finally, we conclude with suggestions for future directions.

II. EXPERIMENTAL

A. Sample fabrication

Substrates were silicon chips of dimension 12.7×12.7 mm. Preparation for deposition was performed in a clean room to minimize the presence of dust particles which could lead to shorts in the Josephson junctions. A multilayer consisting of Nb(150)/PdNi(d_{PdNi})/Nb(25)/Au(15) (with all thicknesses in nanometers) was deposited using magnetically enhanced triode dc sputtering in an Ar plasma pressure of 2.5 mTorr after obtaining a base pressure of 2×10^{-8} Torr or better. A mechanical shadow mask was used to create the multilayer strip of size 0.16×10 mm^2. The thin Au protective layer prevents oxidation of the top Nb layer during further processing steps. The PdNi thickness, d_{PdNi} was varied from 32.5 to 100 nm, typically in 5 nm steps. A subset of samples was fabricated with more closely spaced thicknesses in the range from 58 to 75 nm, in order to demonstrate the minima in critical current indicative of the $0-\pi$ transitions.

The multilayer was patterned using photolithography to create circular photoresist pillars with diameters of 10, 20, 40, and 80 μm on each substrate. Care was taken to ensure the presence of undercut in the resist profile. Either a trilayer photolithography consisting of two photoresist layers separated by a thin metallic layer or a single layer photolithography using chlorobenzene yielded large reliable undercuts in the resist profile. The large variation in area allowed us to have a large dynamic range for the critical current measurements. In practice, however, the success rate of the 80 μm pillars was very low, possibly due to the presence of dust particles during one of the fabrication steps taking place outside the clean room.

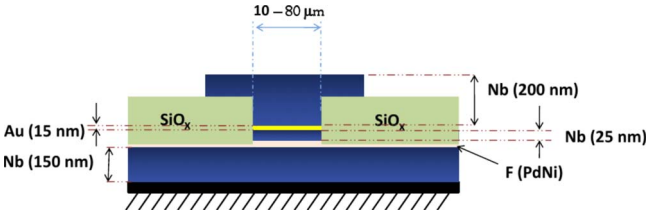

FIG. 1. (Color online) Schematic of a ferromagnetic Josephson junction.

The photoresist pillars acted as a mask to protect the multilayer below them while the rest was ion milled. The multilayer was milled down to the middle of the ferromagnetic layer, thus completely removing the top Nb layer yet not exposing the bottom Nb layer, to prevent the possibility of back-sputtered Nb depositing on the sides of the circular pillars. Nearly 200 nm of SiO_x was then deposited to insulate the bottom Nb from the top Nb leads. Lift off of the photoresist pillars was then done using Remover PG. This was followed by a slight ion milling of the top Au layer to ensure a clean interface. The top Nb lead of thickness 150 nm was then sputtered in the end. The thin Au layer becomes superconducting due to the proximity effect, as it is sandwiched between two Nb layers. A schematic of a complete Josephson junction is shown in Fig. 1.

B. Characterization of PdNi alloy

The Ni concentration of our PdNi alloy was estimated by three different methods. Energy dispersive x-ray analysis (EDAX), performed on a 1.5 μm thick PdNi film, yielded a Ni concentration of $12 \pm 0.5\%$. (A thick film was used for this measurement to increase the signal-to-noise ratio for the Ni-K peak. Similar measurements performed on 200 nm thick PdNi film yielded a similar concentration value provided the signal was accumulated for long enough times.) To corroborate this value for the concentration, the magnetization M vs temperature of a 100 nm thick PdNi film was measured using a Quantum Design superconducting quantum interference device (SQUID) magnetometer (see Fig. 2). A clear change in the slope is seen around the Curie temperature of about 175 K, independent of whether the magnetic field is applied in plane or out of plane. This Curie temperature corresponds to a Ni concentration of 12%, according to earlier work by Beille,[31] cited by Kontos.[32]

Figure 3 shows M vs H at $T=10$ K for the same 100 nm thick PdNi film. The magnetization curve is more rounded, and has smaller remanent magnetization, when the field is

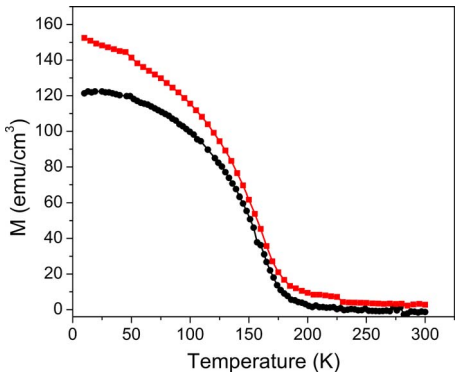

FIG. 2. (Color online) Magnetization vs temperature for a 100 nm thick PdNi film, grown on 150 nm of Nb to have identical crystalline properties as our Josephson junction samples. The film was first cooled in zero field to 10 K, then magnetized by applying an in-plane field (black circles) or out-of-plane field (red squares) of 5 kG, then the magnetic moment was measured in field while heating to room temperature. The cooling curves (not shown) were also measured, and were found to follow the same curves as during heating except for occasional jumps seen for the out-of-plane field case.

applied in plane, indicating that the magnetic anisotropy of PdNi films is out of plane. Similar measurements on PdNi films of thickness 30 and 60 nm also indicate out-of-plane anisotropy, but somewhat less pronounced than in the 100 nm film. The out of plane anisotropy of PdNi surprised us initially, because the strong shape anisotropy of thin films usually dominates over magnetocrystalline anisotropy, resulting in overall in-plane anisotropy. Out-of-plane anisotropy has been observed in several materials, however, including CuNi alloy.[33,34] Recently, we learned that Aprili[35] has also observed out-of-plane anisotropy in PdNi films. The implications of PdNi's out-of-plane anisotropy on our work will be discussed further at the end of this paper.

The saturation magnetization of PdNi measured out-of-plane at 10 K is $M_{\mathrm{sat}}=150$ emu/cm$^3=0.23\mu_B$/atom (see Fig. 3). According to Refs. 31 and 32, this corresponds to a Ni concentration of nearly 12%, in agreement with the determination from the EDAX measurements and Curie temperature.

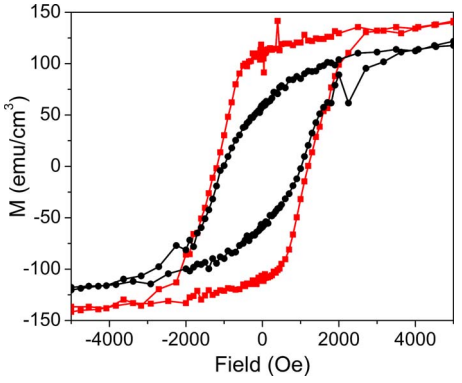

FIG. 3. (Color online) Magnetization vs in-plane field (black circles) and out-of-plane field (red squares) for the same 100 nm thick PdNi film shown in Fig. 2, measured at 10 K.

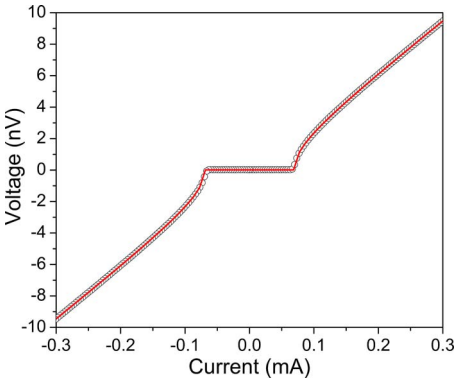

FIG. 4. (Color online) Voltage vs current for a Josephson junction with diameter 20 μm and $d_{\mathrm{PdNi}}=62$ nm and $H_{\mathrm{ext}}=-19$ Oe. The red solid line is a fit to Eq. (1).

C. I_c measurement

The normal-state resistances of our Josephson junction pillars vary from 2.4 to 152 $\mu\Omega$, depending mostly on the pillar area, and, to a lesser extent, on the PdNi thickness. Resistances in this range require an extremely sensitive low noise measurement technique which is provided by using a superconducting quantum interference device as a null detector in a current-comparator circuit.[36] All the four probe measurements were performed at 4.2 K by dipping the probe into a liquid helium dewar equipped with a cryoperm shield. Each chip had Josephson junctions of diameters 10, 20, 40, and 80 μm. All measurements reported here were performed on junctions having Josephson penetration depth, $\lambda_J=\{\Phi_0/[2\pi\mu_0 J_c(d_F+2\lambda_L)]\}^{1/2}$ larger than one-quarter of the junction diameter w. ($\Phi_0=h/2e$ is the superconducting flux quantum, J_c is the critical current density, and λ_L is the London penetration depth, equal to about 86 nm in our sputtered Nb.) This ensures uniform current density in the Josephson junction.[37]

III. CHARACTERIZATION OF JOSEPHSON JUNCTIONS

Figure 4 shows an I-V relation typical for our S/F/S Josephson junctions. The curve follows the standard form for large-area, overdamped junctions,

$$V(I)=\frac{I}{|I|}R_N\,\mathrm{Re}[(I^2-I_c^2)^{1/2}] \qquad (1)$$

Occasionally, we find that the I-V curves are shifted horizontally, so that the critical current is not exactly the same in the positive and negative current directions. In such cases, we average the critical currents in the two current directions.

One of the best ways to characterize Josephson junctions is to observe the modulation of critical current as a function of magnetic field H_{ext} applied perpendicular to the current flow direction in the junction. In nonmagnetic square junctions, the pattern so obtained is called the Fraunhofer pattern, due to its similarity to the pattern produced in single-slit diffraction of light. Observation of a good Fraunhofer pattern demonstrates that the supercurrent is uniform across the junction area, and that there are no short circuits in the surrounding SiO_x insulator.

In nonmagnetic Josephson junctions with circular cross section and negligible screening ($\lambda_J > w$), the magnetic-field dependence of the critical current is given by

$$I(\Phi) = I_c(0)\frac{2 \times J_1\left(\frac{\pi\Phi}{\Phi_0}\right)}{\left(\frac{\pi\Phi}{\Phi_0}\right)}, \quad (2)$$

where $I_c(0)$ is the critical current in the absence of magnetic field, J_1 is the Bessel function of the first kind of order 1, and $\Phi = H_{\text{ext}}(2\lambda_L + d)w$ is the magnetic flux penetrating the middle of the Josephson junction, with λ_L the London penetration depth, w the diameter of the circular junction, and d the thickness of the barrier. This pattern is called an "Airy pattern." The pattern is qualitatively similar to the Fraunhofer diffraction pattern, but the first minima are spaced more widely apart in field than the subsequent minima.

In samples containing a ferromagnetic barrier, one must include the intrinsic flux of the magnetic barrier on the Fraunhofer pattern. If the magnetization M is uniform throughout the junction, the intrinsic magnetic flux is given by $\Phi_F = \mu_0 M d_F w$, with d_F the F-layer thickness and w the cross section width (equal to the diameter for circular junctions). In that case, the total magnetic flux through the F layer is given by

$$\Phi_{\text{tot}} = \mu_0 M d_F w + H_{\text{ext}}(2\lambda_L + d_F)w. \quad (3)$$

In macroscopic samples the magnetization breaks into domains, and Eq. (3) is not valid. Instead, one must integrate the current density across the area of the junction, taking into account the spatial dependence of the magnetic vector potential $\vec{A}$ due to the domains. In the Coulomb gauge, one takes $\vec{A}$ pointing along the current direction (taken as $\hat{z}$). The gauge-invariant phase difference across the junction includes a term proportional to the line integral of $\vec{A}$ from deep inside one superconducting contact to deep inside the other.[38] The resulting expression for the supercurrent is

$$I_s = \int J(x,y)dxdy, \quad (4)$$

where

$$J(x,y) = J_c \sin\left(\alpha + \frac{e}{\hbar c}\int \mathbf{A}(\mathbf{x},\mathbf{y}) \cdot \mathbf{dl}\right). \quad (5)$$

The term containing the vector potential performs a random walk as one moves across the sample, due to the domains pointing in random directions. If the magnetic domains are very small and/or the magnetization is very weak, then the vector potential term stays near zero in all parts of the junction, and the critical current is hardly affected. If, however, the magnetic domains are large and/or have large magnetization as in the case of strong ferromagnet, the contribution to the phase due to the vector potential deviates far from zero as it crosses even a single domain, thus severely suppressing the critical current. This can lead to complete destruction of the Fraunhofer pattern. This is clearly seen in Fig. 5, which shows data for an S/F/S junction of diameter 10 μm, with an 11 nm thick Ni layer. (Similar random-looking "Fraunhofer patterns" have also been seen by other groups studying S/F/S Josephson junctions.[39]) In principle, a regular Fraunhofer pattern can be recovered if the sample is completely magnetized, by applying a magnetic field in the opposite direction to the magnetization such that the total flux given by Eq. (3) is zero. In that case, one should observe a regular Fraunhofer pattern shifted in field by an amount,

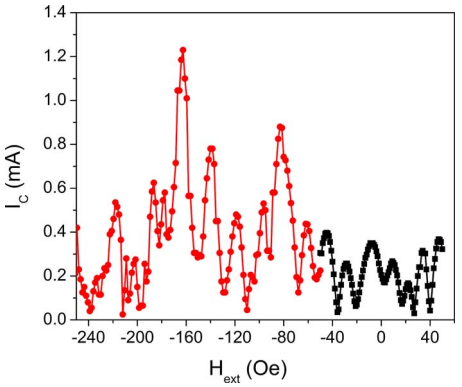

FIG. 5. (Color online) Critical current vs in-plane magnetic field for a Nb/Ni/Nb circular Josephson junction of diameter 10 μm, with $d_{\text{Ni}} = 11$ nm. The black points (squares) were measured in the virgin state, whereas the red points (circles) were measured after magnetizing the sample in an external field of +1 kOe. The random pattern arises due to the intrinsic magnetic flux of the complex domain structure of the Ni layer.

$$H_{\text{shift}} = \frac{-\mu_0 M d_F}{(2\lambda_L + d_F)}. \quad (6)$$

The above argument holds only if the coercive field of the magnetic material is large enough so that the magnetization stays nearly uniform even in the presence of the applied field, H_{shift}, pointing in the opposite direction. For the case of the Ni sample shown in Fig. 5, the largest peak in the critical current vs field after magnetization is found near 160 Oe, whereas the expected shift calculated from the known saturation magnetization of Ni is about 207 Oe. The discrepancy is caused by some rotation of the magnetization in the domains or some domain wall motion as H_{ext} approaches the coercive field, which we measured to be approximately 180 Oe in a separate 9 nm Ni film.

To avoid the distortion of the Fraunhofer pattern, there are several options for the study of ferromagnetic Josephson junctions: (1) use ultrathin samples: under this condition the flux enclosed in the junction due to a single magnetic domain is much less than one flux quantum, and one can safely ignore the contribution to the flux from the magnetization. This option is not available to us, because our goal requires us to work with thick ferromagnetic layers. In addition, thin magnetic films often have magnetically "dead" layers on each side, which pose additional problems for ultrathin samples. (2) Use samples with ultrasmall lateral dimensions to reduce the contribution to the total magnetic flux from the magnetization, and to control the domain structure: this method has been pursued by Robinson *et al.*[40] and also by Sürger *et al.*,[41]

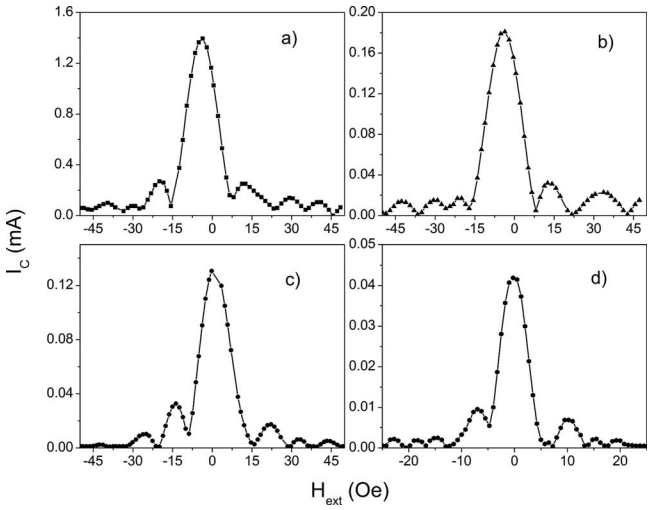

FIG. 6. Critical current vs applied magnetic field (Fraunhofer patterns) obtained for Nb/PdNi/Nb Josephson junctions with different thickness of PdNi interlayer (a) 35 nm, (b) 50 nm, (c) 70 nm, and (d) 85 nm. The pillar diameters w are 10, 10, 10, and 20 μm, respectively.

using strong ferromagnets. The disadvantage of this approach is that it becomes less effective as the thickness of the ferromagnetic layer is increased. In addition, it restricts the possibilities to introduce magnetic inhomogeneities that are naturally present due to the domain structure in devices of larger dimension, and which may be crucial for inducing the predicted spin-triplet superconducting correlations discussed in Sec. I. (3) Work with materials that either have weak magnetization, small domain size, or both: As discussed previously, this approach has been used by Ryazanov and co-workers[8,29] who worked with CuNi alloy, and by Kontos *et al.*,[23] who worked with PdNi alloy. In CuNi alloy, Ryazanov demonstrated that the magnetization of the CuNi makes very little contribution to the total magnetic flux in his samples.[42] He did this by comparing the Fraunhofer pattern for a demagnetized sample with the pattern for the same sample uniformly magnetized. The latter pattern was shifted by a constant field, while the maximum value of the critical current was nearly unchanged. That shows that the integrated vector potential stayed close to zero everywhere in the sample. (4) Engineer the F layer to have zero net magnetic flux, for example, by using a "synthetic antiferromagnet." We are currently exploring this option, and will report it in a future publication.[43]

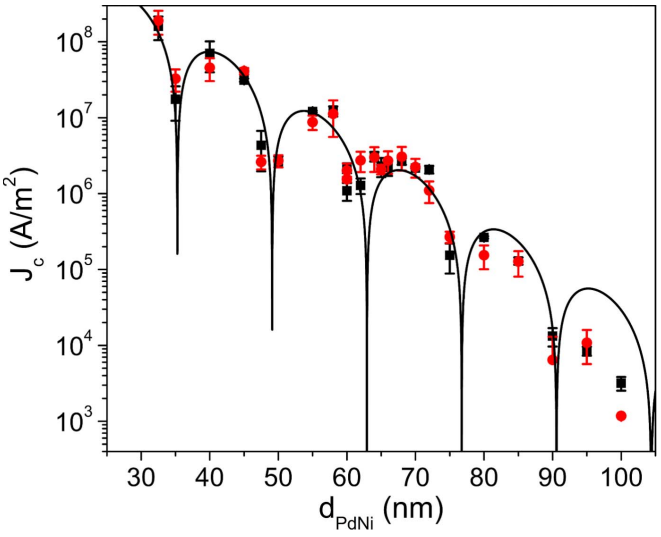

FIG. 7. (Color online) Critical current density vs d_{PdNi} for all of our Nb/PdNi/Nb Josephson junctions. Each data point represents the average over multiple pillars on the same substrate, with the error bars as the standard deviation. Black points (squares) are virgin state data, while red points (circles) were measured after magnetizing the samples (see Fig. 10). The solid line is a fit of Eq. (9) to the virgin state data, while ignoring the last two data points with d_{PdNi}=95 and 100 nm.

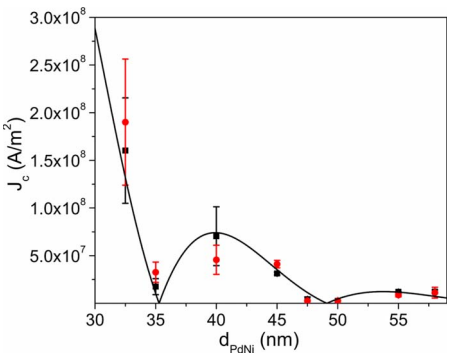

FIG. 8. (Color online) Linear plot of J_c vs d_{PdNi} for the thickness range 32.5–58 nm. The line is the same fit shown in Fig. 7.

For this work, we have chosen the third option, but with PdNi alloy rather than CuNi alloy as our weak ferromagnet. As discussed in Sec. I, there is evidence of strong spin-flip scattering in CuNi alloy, whereas the situation in PdNi alloy is less clear. It should be emphasized that the magnetism in PdNi is quite different from the magnetism in CuNi. Because Pd is nearly ferromagnetic itself according to the Stoner criterion, it takes only a small concentration of Ni to make the alloy ferromagnetic. One might expect then that the magnetism is more uniform in PdNi than in CuNi, where magnetism results from large Ni clusters.[44,45]

As a final note regarding Nb/PdNi/Nb junctions, we found that using PdNi layers thinner than 30 nm resulted in very large critical current densities—so large that even our smallest pillars (w=10 μm) were in the regime $\lambda_J \ll w$. Kontos *et al.*[23] circumvented that problem by introducing an additional insulating layer in their junctions to reduce J_c and hence increase λ_J. Because our interest is in studying junctions with large d_F, we omitted the insulating layer. This choice limited our study to junctions with $d_F > 30$ nm, which have small enough J_c so that $\lambda_J > w/4$ for our smallest diameter pillars.

IV. S/F/S JOSEPHSON JUNCTIONS WITH PdNi: RESULTS

Figure 6 shows I_c vs H_{ext} data for Nb/PdNi/Nb Josephson junctions with 35, 50, 70, and 85 nm of PdNi. The critical current has minima whenever an integer number of flux quanta penetrate the junction. The extremely low values of

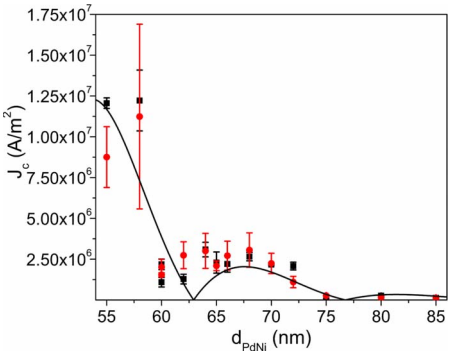

FIG. 9. (Color online) Linear plot of J_c vs d_{PdNi} for the thickness range 55–85 nm. The line is the same fit shown in Fig. 7.

critical current at the minima indicate the absence of any shorts in the insulating material surrounding the Josephson junctions. Similar measurements were performed on samples for which the PdNi thickness varied from 35 to 100 nm. The maximum current density, J_c, obtained for all such devices is plotted vs thickness in Fig. 7. This figure represents the main result of this work. The error bars represent the standard deviation of the results obtained from several pillars on the same substrate. (For the smaller values of d_{F}, we measured primarily the pillars of diameter 10 and 20 μm, whereas for the larger values of d_{F}, we measured the 20 and 40 μm pillars.) The critical current density decreases exponentially over 5 orders of magnitude over this range of PdNi thickness. To our knowledge, these data represent the widest range of ferromagnet thickness in S/F/S Josephson junctions studied to date.

Figure 7 shows that J_c does not decrease monotonically with d_{F}, but rather exhibits local minima with d_{F} in the neighborhood of 35, 48, 60, and 75 nm. Figures 8 and 9 show J_c vs d_{F} on linear axes, where the local minima are clearer. Such local minima have been observed in S/F/S junctions made with several different ferromagnetic materials,[8,10,23,46–50] and signify transitions between standard junctions and π junctions.

Measurements of I_c vs H_{ext} were also performed on the samples after magnetizing them by applying an in-plane field of 5 kOe. The resulting Fraunhofer patterns (see Fig. 10) are shifted in field to a point where the flux due to the external field cancels out the flux due to the intrinsic magnetization. The maximum critical currents obtained for magnetized samples match closely with the virgin state data. This indicates that the domains in PdNi alloy are relatively small, so that the total excursion of the integrated vector potential as one crosses a domain is much less than one flux quantum.

Figure 11 shows the field shift of the Fraunhofer pattern of the magnetized samples vs PdNi thickness d_{F}. As d_{F} increases, the field shift saturates at a value near 200 Oe. As the PdNi thickness increases, there is an increasing tendency for the magnetization to rotate out of the plane, thereby decreasing its in-plane component. The solid line is a fit to the data of Eq. (6), with the only free parameter being the remanent magnetization $M=55$ emu/cm^3. This compares with values of 76 and 62 emu/cm^3 measured directly on PdNi films of thickness 30 and 60 nm, respectively. The red stars

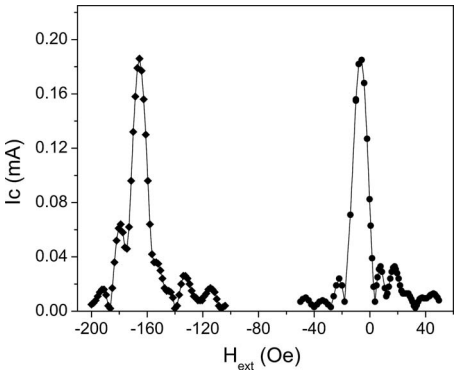

FIG. 10. Fraunhofer pattern in the virgin state (right) and after magnetizing (left) a Nb/PdNi/Nb Josephson junction with diameter $w=10$ μm and $d_{\mathrm{PdNi}}=47.5$ nm.

in Fig. 11 show the values of H_{shift} calculated from Eq. (6), using the values of M_{rem} measured directly on PdNi films of thickness 30, 60, and 100 nm. The agreement with the field shifts of the Fraunhofer patterns is reasonable.

We have also measured the normal-state resistance of our samples at currents much larger than I_c. A plot of the specific resistance AR_N (area times resistance) vs d_{PdNi} is shown in Fig. 12. The interface and bulk contributions to AR_N are given by

$$AR_N = 2AR_B + \rho_{\mathrm{PdNi}} d_{\mathrm{F}}, \tag{7}$$

where ρ_{PdNi} is the resistivity of PdNi, d_{F} is the thickness of the PdNi layer, and R_B is the Nb/PdNi boundary resistance. A linear fit to all of the data gives a boundary resistance of $AR_B=2.31\pm0.07$ fΩ m^2 and a resistivity of PdNi, $\rho_{\mathrm{PdNi}}=68\pm3$ nΩ m. Independent measurements of the in-plane PdNi resistivity were performed on 200 nm thick films, using the van der Pauw method. Those measurements produced the value $\rho_{\mathrm{PdNi}}=116\pm2$ nΩ m. It is plausible that the in-plane

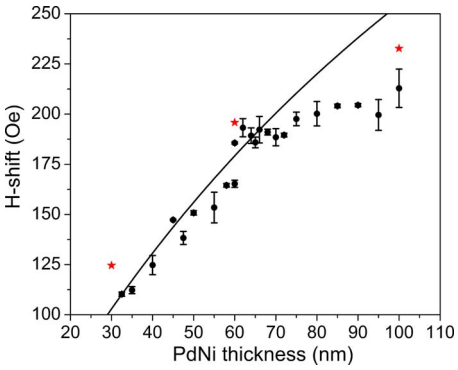

FIG. 11. (Color online) Magnetic field shift of Fraunhofer patterns of magnetized samples vs PdNi thickness d_{F}. Error bars are the standard deviation from several pillars on the same substrate. The line is a fit of Eq. (6) to the data points with $d_{\mathrm{F}}<75$ nm, with $\lambda_L=86$ nm. The fit provides an estimate of 55 emu/cm^3 for the remnant magnetization M_{rem} of PdNi alloy. The red stars indicate the calculated H_{shift} using values of M_{rem} measured in a SQUID magnetometer on PdNi films of thickness 30, 60, and 100 nm. (Fig. 3 shows the M vs H data for the 100 nm film.)

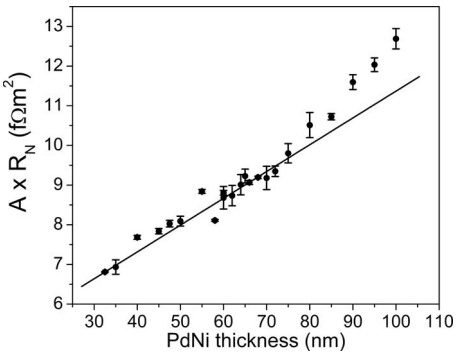

FIG. 12. Area times normal-state resistance vs d_{PdNi} for all of our Josephson junction samples. Error bars are the standard deviation from measurements of several pillars on the same substrate. The slope of the linear fit provides the resistivity of PdNi and the y intercept provides twice the Nb/PdNi boundary resistance.

resistivity is larger than the perpendicular resistivity if the PdNi films grow in a columnar fashion, although measurements on other sputtered metals often find quite close agreement between these two measurement methods.[51]

V. THEORY OF S/F/S JOSEPHSON JUNCTIONS

There have been a large number of theoretical works dealing with S/F/S Josephson junctions. There are three energy scales whose relative size determines three distinct regimes. The energy scales are the exchange energy in the ferromagnet, E_{ex}, the gap in the superconductor, Δ, and $\hbar/\tau$, where τ is the mean-free time between collisions of an electron propagating in the ferromagnet. In all of the experimental work on S/F/S Josephson junctions published to date, including this work, $E_{\mathrm{ex}} \gg \Delta$. There is a wide variation, however, in the size of $\hbar/\tau$ relative to those two energies. The true clean limit is expressed by $E_{\mathrm{ex}}\tau \gg \hbar$, which also implies $\Delta\tau \gg \hbar$. The intermediate limit is where $E_{\mathrm{ex}}\tau > \hbar$ but $\Delta\tau < \hbar$, whereas the true dirty limit is where both $\Delta\tau \ll \hbar$ and $E_{\mathrm{ex}}\tau \ll \hbar$. These three regimes can also be characterized by the relative sizes of the three length scales: the electron mean-free path, $l_e = v_F\tau$, the superconducting coherence length, $\xi_S = \hbar D_S/\Delta$, and the clean-limit exchange length discussed earlier, $\xi_F = \hbar v_F/2E_{\mathrm{ex}}$.

The simplest limit is the dirty limit, with the additional constraint that the ferromagnetism is weak enough so that one can treat the spin-up and spin-down bands identically, i.e., as having the same Fermi velocity and mean-free path. In this limit, the Usadel equation is valid. An expression for the critical current I_c as a function of ferromagnetic layer thickness d_{F} was first derived by Buzdin *et al.*[52] In this regime, the oscillation and decay of I_c as a function of d_{F} are both governed by a single length scale—the "dirty-limit" exchange length, $\xi_F^* = (\hbar D_F/E_{\mathrm{ex}})^{1/2}$. Once d_{F} exceeds ξ_F^*, the thickness dependence of I_c takes the simple form,

$$I_c(d_{\mathrm{F}}) = I_{c0} \exp\left(\frac{-d_{\mathrm{F}}}{\xi_F^*}\right) \left| \sin\left(\frac{d_{\mathrm{F}}}{\xi_F^*} + \pi/4\right) \right|. \tag{8}$$

In the presence of spin-flip or spin-orbit scattering, Eq. (8) is modified, and the length scales governing the decay and the oscillation are no longer equal.[9,14,30,53,54] The more general form can be written as

$$I_c(d_{\mathrm{F}}) = I_{c0} \exp\left(\frac{-d_{\mathrm{F}}}{\xi_{F1}}\right) \left| \sin\left(\frac{d_{\mathrm{F}}}{\xi_{F2}} + \phi\right) \right|. \tag{9}$$

In general, the effect of spin-flip or spin-orbit scattering is to shorten the decay length scale, ξ_{F1}, relative to ξ_F^*, and to lengthen the oscillation length scale, ξ_{F2}. In the presence of sufficiently strong spin-orbit (but not spin-flip) scattering, the oscillations disappear completely. An equation similar to Eq. (9) has successfully been used to fit I_c vs d_F data from S/F/S junctions containing CuNi alloy, with $\xi_{F1} = 1.3$ nm, and $\xi_{F2} = 3.5$ nm.[8] The very short value of ξ_{F1} compared to ξ_{F2} was interpreted as implying that spin-flip scattering is strong in that material.

Equation (9) can also be fit to our data, as shown in Figs. 7–9. But in our case, the length scale governing the exponential decay ($\xi_{F1} = 7.7 \pm 0.5$ nm) is considerably longer than the length scale governing the oscillation ($\xi_{F2} = 4.4 \pm 0.1$ nm), hence the dirty-limit hypotheses that led to Eq. (9) are not fulfilled. However, the condition $\xi_{F1} > \xi_{F2}$ has also observed in S/F/S Josephson junctions containing the strong ferromagnets: Ni, Fe, Co, and $Ni_{80}Fe_{20}$ (also known as Permalloy, or Py).[10] Those materials have very large exchange energy, hence they are in the intermediate limit, with $E_{\mathrm{ex}}\tau > \hbar$ but still $\Delta\tau < \hbar$. Our observation of $\xi_{F1} > \xi_{F2}$ in S/F/S junctions with PdNi alloy suggest that PdNi may also be in the intermediate limit.

The intermediate limit has been studied in several theoretical papers. Bergeret *et al.*[11] provide a general formula for the critical current, valid both in the dirty limit and intermediate limit. In the intermediate limit the formula simplifies when the F-layer thickness is larger than the mean-free path. Equation (20) from Ref. 11 is

$$I_c(d_{\mathrm{F}}) \propto \pi T \sum_{\omega>0} \frac{\Delta^2}{\Delta^2 + \omega^2} \frac{\sin(d_{\mathrm{F}}/\xi_F)}{d_{\mathrm{F}}/\xi_F} \exp\left(\frac{-d_{\mathrm{F}}}{l_e}(1 + 2\omega\tau)\right), \tag{10}$$

where the sum is over the positive Matsubara frequencies, $\omega_m = \pi k_B T(2m+1)$ with T the temperature. Asymptotically at large values of d_{F}, Eq. (10) is quite similar to Eq. (9), with $\xi_{F1} = l_e$ and $\xi_{F2} = \xi_F$. Nevertheless, we have fit Eq. (10) directly to our data, and obtained the parameters $\xi_F = 4.0 \pm 0.1$ nm and $l_e = 10.6 \pm 1$ nm. The former is close to the value of ξ_{F2} obtained from the fit of Eq. (9), while the value of l_e obtained from Eq. (10) is somewhat larger than the value of ξ_{F1} obtained from the fit of Eq. (9)—the difference undoubtedly due to the sum over Matsubara frequencies in Eq. (10). We will use the larger value of l_e in the following discussion.

An alternative theoretical approach was taken by Kashuba *et al.*[55] who considered a model of S/F/S junctions taking explicit account of spin-dependent and spin-flip scattering in the F layer. In the intermediate limit, these authors find a result that is nearly identical to Eq. (10).

VI. DISCUSSION OF RESULTS

A. Estimate of mean-free path and exchange energy in PdNi

In many metals, it is straightforward to estimate the mean-free path directly from the measured resistivity, as the product ρl_e is inversely proportional to the Fermi surface area, and has been tabulated for a large number of metals.[56] In PdNi alloy, however, the ρl_e product is not known. Some workers have tried to estimate ρl_e in PdNi from its value in Pd, but even that estimation is not straightforward, due to the complex band structure of Pd. To illustrate the difficulty, previous workers have quoted values of the ρl_e product as small as 0.33 fΩ m^2 (Refs. 24 and 25) and as large as 4.0 fΩ m^2 (Ref. 32). The former value is certainly too small, because it was calculated using the Einstein relation, $\sigma = n(E_F)e^2D$, with the density of states at the Fermi level, $n(E_F)$, obtained from the electronic specific heat coefficient $\gamma = (\pi^2/3)k_B^2 n(E_F)$. The problem is that, in Pd, the specific heat is dominated by heavy holes on the open "jungle gym" portion of the Fermi surface, while the electronic transport is dominated by much lighter electrons on a part of the surface centered at the Γ point. (It is common to refer to these electrons as "s-like;" but that is incorrect because they are strongly hybridized with the d bands.[57]) Discussion of the Fermi surface in Pd has been given in several papers.[57–60] Pinski *et al.*[57] state that the Γ-centered sheet of the Fermi surface carries the vast majority of the transport current—up to 97% at 10 K.

We estimate the ρl_e product for PdNi in two ways. In his Ph.D thesis,[32] Kontos found that the resistivity of thin PdNi films with $x \approx 12\%$ varied linearly with inverse thickness $1/d$ once the films were thinner than about 8 nm, indicating that the mean-free path is limited by the film thickness. The slope of the graph gives the product $\rho d = 1.7$ fΩ m^2. Typical polycrystalline films have mean-free paths within a factor of 2 of the film thickness; hence we expect ρl_e to be within a factor of 2 this value. The second method relies on the statement by Pinksi *et al.*[57] that electronic transport in Pd is dominated by the electrons on the Γ-centered sheet. The total number of carriers in that band, the density of states at the Fermi level, the effective mass, and the Fermi velocity on that sheet have all been tabulated by Dye *et al.*[59] based on de Haas van–Alphen measurements of the Fermi surface of Pd. The values of those four quantities are: $n = 0.375$ carriers/atom $= 2.54 \times 10^{28}$ m^{-3}; $n(E_F) = 0.189$ states/(eV atom spin) $= 2.56 \times 10^{28}$ eV^{-1} m^{-3}; $m^* = 2.0 m_e$; and $v_F = 0.6(2\pi/a)\cdot(\hbar/2m) = 5.6 \times 10^5$ m/s. Using the Drude formula, $\sigma = ne^2\tau/m^*$, one finds $\rho l_e = 1.55$ fΩ m^2, while using the Einstein relation one finds $\rho l_e = 1.31$ fΩ m^2. (The slight difference between the two values is likely due to the nonparabolic character of the Γ-centered sheet.) These values are close to the value $\rho l_e = 1.7$ fΩ m^2 estimated from the thickness dependence found by Kontos. If we take our own measured resistivity, $\rho = 68$ nΩ m, and the value of the mean-free path from the J_c vs d_F fit, $l_e = 10.6$ nm, we obtain $\rho l_e = 0.72$ fΩ m^2, which is not too far from the estimates given above. (The only mystery we cannot explain from this analysis is the very low value of the Fermi velocity, $v_F = 2.0 \cdot 10^5$ m/s, measured by Dumoulin *et al.*[61] in a proximity effect experiment between Pb and Pd. It is unclear why that experiment measures the low Fermi velocity of the open hole sheet rather than the higher Fermi velocity of the Γ-centered sheet.)

From the period of oscillation of J_c vs d_F, we found $\xi_{F2} = 4.4 \pm 0.1$ nm. Using the Fermi velocity of the dominant carriers, $v_F = 5.6 \cdot 10^5$ m/s, gives an estimate for the exchange energy in our $Pd_{88}Ni_{12}$ alloy of $E_{ex} = \hbar v_F / 2\xi_{F2} = 42$ meV. This value is somewhat higher than values quoted by previous workers,[23–27] but those earlier estimates were either made using the smaller value of v_F, or using the diffusive formula $\xi_F^* = \sqrt{(\hbar D / E_{ex})}$. A more meaningful comparison is of the length scales ξ_{F1} and ξ_{F2} found in different experiments. For example, Kontos *et al.*[23] found $\xi_{F1} \approx \xi_{F2} = 2.8$ nm in their study of S/I/F/S Josephson junctions with a PdNi alloy of similar concentration to ours. The values of ξ_{F2} in their experiment and ours are rather close to each other, but the values of ξ_{F1} are not. It is not clear if that discrepancy is significant or not. The thickness range covered in the earlier work was 4.5–14 nm, whereas the range we covered was 32.5–100 nm. If the mean-free path in the PdNi alloy is indeed in the range of 10.6 nm, then the samples studied by Kontos *et al.* were in the crossover regime with $d_F \approx l_e$, where the thickness dependence has not yet obtained the asymptotic exponential decay, $J_c \propto \exp(-d_F/l_e)$. But then one would expect a less-steep decay of J_c with d_F, rather than a more steep decay. Perhaps a more relevant observation is simply that the PdNi films deposited in different laboratories may have different polycrystalline structures, and hence very different mean-free paths. A summary of the parameters estimated by previous workers, as well as by our work, is given in Table I.

B. Spin-triplet superconducting correlations?

One of the primary goals of this work was to search for signs of spin-triplet superconducting correlations in our samples. At first glance, the data in Fig. 7 show no sign of spin-triplet superconducting correlations, which might manifest themselves as a crossover to a less-steep exponential decay of J_c at large values of d_F. It is intriguing, however, that the length scale characterizing the exponential decay of J_c in our samples, $\xi_{F1} = 7.7 - 10.6$ nm, is substantially longer than that observed previously in shorter S/F/S junctions with PdNi.[23] Could it be that we are already observing the triplet Josephson effect throughout the whole range of d_F reported here? The strongest evidence against such an interpretation is the nearly periodic set of local minima we observe in J_c vs d_F, shown in Figs. 7–9. We believe that those local minima signal crossovers between 0 junctions and π junctions, which are due to the effect of the exchange splitting on spin-singlet superconducting correlations. A Josephson supercurrent dominated by spin-triplet correlations would not exhibit such minima, but rather would decay monotonically with increasing d_F. Nevertheless, to rule out the spin-triplet hypothesis definitively would require stronger evidence that the local minima we observe truly represent $0-\pi$ crossovers, rather than an unlucky distribution of uncertainties in the data that mimics a periodic set of local minima.

There are three ways one could make a more stringent test that the local minima observed in our J_c vs d_F data are due to

TABLE I. PdNi parameters from several groups. The superconductor used in all the above experiments was Niobium. Note that most workers have used the diffusive formula, $\xi_{F2}=(\hbar D/E_{ex})^{1/2}$, to extract E_{ex} from the measured value of ξ_{F2}, whereas we have used the ballistic formula, $\xi_{F2}=\hbar v_F/2E_{ex}$. Our choice of Fermi velocity, v_F, is discussed in the text.

Source	Expt.	Ni concentration (at. %)	v_F (10^5 m/s)	ρl_e (fΩ m^2)	ρ (nΩ m)	l_e (nm)	ξ_{F1} (nm)	ξ_{F2} (nm)	E_{ex} (meV)	Formula to extract E_{ex}	T_{Curie} (K)
22	S/F DOS	10	2.0	4		$\approx d_F$	2.8	2.8	35	$(\hbar D/E_{ex})^{1/2}$	100
23	S/I/F/S	12	2.0	4		$\approx d_F$	3.5	3.5	13	$(\hbar D/E_{ex})^{1/2}$	260
25	T_c of S/F	14	2.0	4	240	16.6	6	6	15	$(\hbar D/E_{ex})^{1/2}$	156
26,27	T_c of S/F	14	2.0	0.96	240	4	3.4	3.4	13	$(\hbar D/E_{ex})^{1/2}$	185
24	T_c of S/F	15	2.0	0.3256	220	1.48	3.5	3.5	13	$(\hbar D/E_{ex})^{1/2}$	260
28	S/F/S	18	2.0				2.4	2.4	52	$(\hbar D/E_{ex})^{1/2}$	200
This work	S/F/S	12	5.6	0.72	68	10.6	7.7	4.4	42	$\hbar v_F/2E_{ex}$	175

$0-\pi$ crossovers: (1) a direct measurement of the current-phase relationship of the junction.[62] (2) Extension of J_c vs d_F measurements to smaller values of d_F, to see if the slope of the J_c vs d_F semilogarithmic plot changes to a value close to that measured by Kontos *et al.* This would require reducing the lateral size w of our junctions, so as to maintain the condition $\lambda_J > w/4$. (3) Measurement of J_c vs temperature T for samples very close to a $0-\pi$ crossover. In S/F/S junctions with very weak ferromagnets, the $0-\pi$ crossover has been observed in the T dependence of J_c.[8,29,47,50] As the exchange energy increases, however, the thickness range over which one can see a nonmonotonic T dependence of J_c gets progressively narrower.[50] Each of these checks presents its own set of challenges, and represents a possible direction for future work.

C. Spin-flip scattering in PdNi

Assuming that our data are not the result of spin-triplet correlations, we would like to know why not. There are several factors that may contribute. First and foremost, strong spin-flip or spin-orbit scattering, if they exist in our PdNi alloy, would destroy the triplet correlations.[63] To address this issue, we have independently measured the spin memory length, l_{sf}, in PdNi alloy using techniques borrowed from the giant magnetoresistance (GMR) community. A complete discussion of those measurements is given elsewhere.[64] Here we note the most salient results. First, the value of the spin memory length obtained, $l_{sf}=2.8$ nm, is surprisingly short given the much longer length scale characterizing the decay of the Josephson supercurrent in the present work. Normally, one assumes that spin-flip and spin-orbit scattering processes occur on length scales much longer than the mean-free path, justifying the diffusive model used in discussing the spin memory length.[65] In addition, the analysis of the spin-valve data normally assumes that the magnetizations of the two magnetic layers are either parallel or antiparallel to each other. Our recent discovery of the out-of-plane magnetic anisotropy in PdNi casts doubt on this assumption. We now believe that the very short value of l_{sf} measured using a GMR spin valve,[64] as well as the out-of-plane magnetic anisotropy of PdNi, are both due to strong spin-orbit coupling of Ni impurities in Pd studied 30 years ago.[66,67] Due to local strains, the PdNi magnetization may be inhomogeneous on very short length scales, which may then destroy spin memory by rotating the spin on a length scale smaller than the mean-free path. What is perhaps more surprising is that the superconducting spin-singlet pair correlations decay over a length scale four times as long. Clarifying this issue will require further experiments.

A second possible reason we do not observe signs of spin-triplet superconducting correlations is that the length scale characterizing the magnetic inhomogeneity in PdNi might not be comparable to the Cooper pair coherence length ξ_s in Nb. Let us refer to the length scale characterizing the magnetic inhomogeneity as δ_m. If $\delta_m \ll \xi_s$, then a Cooper pair will experience the magnetization averaged over the length ξ_s, and triplet correlations will not be produced efficiently. If $\delta_m \gg \xi_s$, then a typical Cooper pair experiences no magnetic inhomogeneity. The coherence length in our Nb is known to be about 13 nm.[7] Unfortunately, the typical domain sizes and domain wall widths in our PdNi alloy are not known. Because the Curie temperature of PdNi is well below room temperature, obtaining information about magnetic structure requires a low-temperature magnetic visualization technique, such as low-temperature magnetic force microscopy (MFM) or Bitter decoration. And even then, the former method is not well suited to weak ferromagnets, because the magnetization of the MFM tip may influence the domain structure of the sample. Very recently the domain structure of CuNi alloy was measured using the Bitter decoration technique.[34] Those measurements confirmed the out-of-plane magnetic anisotropy of that material, and found a typical domain size of 100 nm in the virgin state or at the coercive field. Unfortunately, no such measurements have been performed on PdNi alloy, to our knowledge. Clearly, a thorough study of the magnetic domain structure of PdNi would help clarify this issue.

VII. FUTURE DIRECTIONS

The most urgent work needed in the future is a strong verification (or repudiation) that the local minima in our data do indeed represent $0-\pi$ crossovers, rather than sample-to-sample fluctuations. Looking further ahead, to have any hope of nailing down the elusive spin-triplet supercurrent in S/F/S junctions will require better characterization of magnetic ma-

terials. On the one hand, the spin diffusion length is a crucial parameter, as it limits the spatial extent of spin-triplet correlations. Fortunately, the spin-diffusion length has been measured in some ferromagnetic materials,[68] but more work is needed. Of equal important is information about the typical length scales characterizing the domain structure of ferromagnetic thin films. This is a complex issue, as either the domain size or domain wall width may be important. For example, in a film where neighboring domains have antiparallel magnetization, the long-range triplet component is generated only in the domain walls,[69] hence it is crucial that the domain wall width be comparable to ξ_s. If, however, neighboring domains have noncollinear magnetizations, then it would seem that the long-range triplet could be produced even if the domain walls are very thin, as long as the typical domain size is comparable to ξ_s. Unfortunately, domain sizes in polycrystalline films are not known *a priori*.[70]

VIII. CONCLUSIONS

We have measured the critical current of Nb/PdNi/Nb Josephson junctions with PdNi thicknesses ranging from 32.5 to 100 nm. The critical current drops by 5 orders of magnitude over this thickness range. The data appear to have a periodic array of local minima, suggesting that the supercurrent is of the conventional spin-singlet type over the entire thickness range. We have discussed possible reasons for the absence of induced spin-triplet correlations, such as spin-flip scattering or a poor match of length scales between the magnetic domains and the superconducting coherence length.

ACKNOWLEDGMENTS

We are grateful to M. Aprili, Y. M. Blanter, I. A. Campbell, T. Kontos, V. V. Ryazanov, and S. K. Yip for helpful discussions, and to B. Bi, R. Loloee, and Y. Wang for technical assistance. We acknowledge the use of the W. M. Keck Microfabrication Facility at Michigan State University. This work was supported by the Department of Energy under Grant No. DE-FG02-06ER46341.

*birge@pa.msu.edu

[1] P. G. de Gennes, Rev. Mod. Phys. **36**, 225 (1964).
[2] C. J. Lambert and R. Raimondi, J. Phys.: Condens. Matter **10**, 901 (1998).
[3] B. Pannetier and H. Courtois, J. Low Temp. Phys. **118**, 599 (2000).
[4] A. I. Buzdin, Rev. Mod. Phys. **77**, 935 (2005).
[5] I. F. Lyuksyutov and V. L. Pokrovsky, Adv. Phys. **54**, 67 (2005).
[6] J. S. Jiang, D. Davidovic, D. H. Reich, and C. L. Chien, Phys. Rev. Lett. **74**, 314 (1995).
[7] J. Y. Gu, C.-Y. You, J. S. Jiang, J. Pearson, Ya. B. Bazaliy, and S. D. Bader, Phys. Rev. Lett. **89**, 267001 (2002).
[8] V. A. Oboznov, V. V. Bol'ginov, A. K. Feofanov, V. V. Ryazanov, and A. I. Buzdin, Phys. Rev. Lett. **96**, 197003 (2006).
[9] E. A. Demler, G. B. Arnold, and M. R. Beasley, Phys. Rev. B **55**, 15174 (1997).
[10] J. W. A. Robinson, S. Piano, G. Burnell, C. Bell, and M. G. Blamire, Phys. Rev. Lett. **97**, 177003 (2006).
[11] F. S. Bergeret, A. F. Volkov, and K. B. Efetov, Phys. Rev. B **64**, 134506 (2001).
[12] A. Kadigrobov, R. I. Shekhter, and M. Jonson, Europhys. Lett. **54**, 394 (2001).
[13] A. F. Volkov, F. S. Bergeret, and K. B. Efetov, Phys. Rev. Lett. **90**, 117006 (2003).
[14] F. S. Bergeret, A. F. Volkov, and K. B. Efetov, Phys. Rev. B **68**, 064513 (2003).
[15] I. Eremin, D. Manske, S. G. Ovchinnikov, and J. F. Annett, Ann. Phys. **13**, 149 (2004).
[16] F. S. Bergeret, A. F. Volkov, and K. B. Efetov, Rev. Mod. Phys. **77**, 1321 (2005).
[17] M. D. Lawrence and N. Giordano, J. Phys.: Condens. Matter **8**, L563 (1996); **11**, 1089 (1999).
[18] V. T. Petrashov, I. A. Sosnin, I. Cox, A. Parsons, and C. Troadec, Phys. Rev. Lett. **83**, 3281 (1999).
[19] M. Giroud, H. Courtois, K. Hasselbach, D. Mailly, and B. Pannetier, Phys. Rev. B **58**, R11872 (1998).
[20] R. S. Keizer, S. T. B. Goennenwein, T. M. Klapwijk, G. Xiao, and A. Gupta, Nature (London) **439**, 825 (2006).
[21] I. Sosnin, H. Cho, V. T. Petrashov, and A. F. Volkov, Phys. Rev. Lett. **96**, 157002 (2006).
[22] T. Kontos, M. Aprili, J. Lesueur, and X. Grison, Phys. Rev. Lett. **86**, 304 (2001).
[23] T. Kontos, M. Aprili, J. Lesueur, F. Genet, B. Stephanidis, and R. Boursier, Phys. Rev. Lett. **89**, 137007 (2002).
[24] K. Matsuda, H. Niwa, Y. Akimoto, T. Uemura, and M. Yamamoto, IEEE Trans. Appl. Supercond. **17**, 3529 (2007).
[25] C. Cirillo, S. L. Prischepa, M. Salvato, and C. Attanasio, J. Phys. Chem. Solids **67**, 412 (2006).
[26] C. Cirillo, J. Aarts, and C. Attanasio, Phys. Status Solidi C **3**, 3015 (2006) c.
[27] C. Cirillo, S. L. Prischepa, M. Salvato, C. Attanasio, M. Hesselberth, and J. Aarts, Phys. Rev. B **72**, 144511 (2005).
[28] A. Bauer, J. Bentner, M. Aprili, M. L. Della-Rocca, M. Reinwald, W. Wegscheider, and C. Strunk, Phys. Rev. Lett. **92**, 217001 (2004).
[29] V. V. Ryazanov, V. A. Oboznov, A. Yu. Rusanov, A. V. Veretennikov, A. A. Golubov, and J. Aarts, Phys. Rev. Lett. **86**, 2427 (2001).
[30] M. Faure, A. I. Buzdin, A. A. Golubov, and M. Yu. Kupriyanov, Phys. Rev. B **73**, 064505 (2006).
[31] J. Beille, Ph.D. thesis, Université Joseph Fourier, Grenoble, 1975.
[32] T. Kontos, Ph.D. thesis, Université Paris XI, Orsay, 2002.
[33] A. Ruotolo, C. Bell, C. W. Leung, and M. G. Blamire, J. Appl. Phys. **96**, 512 (2004).
[34] I. S. Veshchunov, V. A. Oboznov, A. N. Rossolenko, A. S. Prokofiev, L. Ya. Vinnikov, A. Yu. Rusanov, and D. V. Matveev, Pis'ma Zh. Eksp. Teor. Fiz. **88**, 873 (2008).

[35] M. Aprili (private communication).
[36] D. Edmunds, W. Pratt, and J. Rowlands, Rev. Sci. Instrum. **51**, 1516 (1980).
[37] A. Barone and G. Paterno, *Physics and Applications of the Josephson Effect* (Wiley, New York, 1982).
[38] L. P. Lévy, *Magnetism and Superconductivity* (Springer-Verlag, Berlin, 2000).
[39] O. Bourgeois, P. Gandit, J. Lesueur, A. Sulpice, X. Grison, and J. Chaussy, Eur. Phys. J. B **21**, 75 (2001).
[40] J. W. A. Robinson, S. Piano, G. Burnell, C. Bell, and M. G. Blamire, Phys. Rev. B **76**, 094522 (2007).
[41] C. Sürgers, T. Hoss, C. Schönenberger, and C. Strunk, J. Magn. Magn. Mater. **240**, 598 (2002).
[42] V. V. Ryazanov, Usp. Fiz. Nauk **42**, 825 (1999).
[43] M. Khasawneh, W. P. Pratt, Jr., and N. O. Birge (unpublished).
[44] C. G. Robbins, H. Claus, and P. A. Beck, Phys. Rev. Lett. **22**, 1307 (1969).
[45] K. Levin and D. L. Mills, Phys. Rev. B **9**, 2354 (1974).
[46] Y. Blum, A. Tsukernik, M. Karpovski, and A. Palevski, Phys. Rev. Lett. **89**, 187004 (2002).
[47] H. Sellier, C. Baraduc, F. Lefloch, and R. Calemczuk, Phys. Rev. B **68**, 054531 (2003).
[48] V. Shelukhin, A. Tsukernik, M. Karpovski, Y. Blum, K. B. Efetov, A. F. Volkov, T. Champel, M. Eschrig, T. Löfwander, G. Schön, and A. Palevski, Phys. Rev. B **73**, 174506 (2006).
[49] M. Weides, M. Kemmler, E. Goldobin, D. Koelle, R. Kleiner, H. Kohlshedt, and A. Buzdin, Appl. Phys. Lett. **89**, 122511 (2006).
[50] A. A. Bannykh, J. Pfeiffer, V. S. Stolyarov, I. E. Batov, V. V. Ryazanov, and M. Weides, Phys. Rev. B **79**, 054501 (2009).
[51] S.-F. Lee, Q. Yang, P. Holody, R. Loloee, J. H. Hetherington, S. Mahmood, B. Ikegami, K. Vigen, L. L. Henry, P. A. Schroeder, W. P. Pratt, Jr., and J. Bass, Phys. Rev. B **52**, 15426 (1995).
[52] A. I. Buzdin, B. Bujicic, and B. M. Yu. Kupriyanov, Zh. Eksp. Teor. Fiz. **101**, 231 (1992) [Sov. Phys. JETP **74**, 124 (1992)].
[53] F. S. Bergeret, A. F. Volkov, and K. B. Efetov, Phys. Rev. B **75**, 184510 (2007).
[54] J. Linder, T. Yokoyama, and A. Sudbø, Phys. Rev. B **77**, 174514 (2008).
[55] O. Kashuba, Y. M. Blanter, and V. I. Fal'ko, Phys. Rev. B **75**, 132502 (2007).
[56] J. Bass, in *Metals: Electronic Transport Phenomena*, (Springer-Verlag, Berlin, 1982), pp. 1–288.
[57] F. J. Pinski, P. B. Allen, and W. H. Butler, Phys. Rev. B **23**, 5080 (1981).
[58] J. J. Vuillemin, Phys. Rev. **144**, 396 (1966).
[59] D. H. Dye, S. A. Campbell, G. W. Crabtree, J. B. Ketterson, N. B. Sandesara, and J. J. Vuillemin, Phys. Rev. B **23**, 462 (1981).
[60] I. I. Mazin, E. M. Savitskii, and Yu. A. Uspenskii, J. Phys. F: Met. Phys. **14**, 167 (1984).
[61] L. Dumoulin, P. Nedellec, and P. M. Chaikin, Phys. Rev. Lett. **47**, 208 (1981).
[62] S. M. Frolov, D. J. Van Harlingen, V. A. Oboznov, V. V. Bolginov, and V. V. Ryazanov, Phys. Rev. B **70**, 144505 (2004).
[63] If the spin-orbit scattering rate is larger than $E_{ex}/\hbar$, then I_c does not exhibit oscillations with d_F. The spin-orbit scattering rate we are considering in this discussion is smaller than that.
[64] H. Arham, T. Khaire, R. Loloee, W. P. Pratt, Jr., and N. O. Birge (unpublished).
[65] T. Valet and A. Fert, Phys. Rev. B **48**, 7099 (1993).
[66] L. D. Khoi, P. Veillet, and I. A. Campbell, J. Phys. F: Met. Phys. **6**, L197 (1976).
[67] S. Senoussi, I. A. Campbell, and A. Fert, Solid State Commun. **21**, 269 (1977).
[68] J. Bass and W. P. Pratt, Jr., J. Phys.: Condens. Matter **19**, 183201 (2007).
[69] Ya. V. Fominov, A. F. Volkov, and K. B. Efetov, Phys. Rev. B **75**, 104509 (2007).
[70] R. C. O'Handley, *Modern Magnetic Materials: Principles and Applications* (Wiley, New York, 2000), Chap. 8.